COMMUNICATION

ADVANCED MATERIALS

Polymer Dynamics

www.advmat.de

Liquid-Cell Electron Microscopy of Adsorbed Polymers

*Kandula Hima Nagamanasa, Huan Wang, and Steve Granick**

Individual macromolecules of polystyrene sulfonate and poly(ethylene oxide) are visualized with nanometer resolution using transmission electron microscopy (TEM) imaging of aqueous solutions with and without added salt, trapped in liquid pockets between creased graphene sheets. Successful imaging with 0.3 s per frame is enabled by the sluggish mobility of the adsorbed molecules. This study finds, validating others, that an advantage of this graphene liquid-cell approach is apparently to retard sample degradation from incident electrons, in addition to minimizing background scattering because graphene windows are atomically thin. Its new application here to polymers devoid of metal-ion labeling allows the projected sizes and conformational fluctuations of adsorbed molecules and adsorption–desorption events to be analyzed. Confirming the identification of the observed objects, this study reports statistical analysis of datasets of hundreds of images for times up to 100 s, with variation of the chemical makeup of the polymer, the molecular weight of the polymer, and the salt concentration. This observation of discrete polymer molecules in solution environment may be useful generally, as the findings are obtained using an ordinary TEM microscope, whose kind is available to many researchers routinely.

Time-resolved electron microscopy does not yet match the revolutionary advances that allow one to track single-molecular trajectories and interactions of organic molecules in solution using optical microscopy,[1] despite the fact that its resolution is potentially higher because wavelengths are orders of magnitude less than for light. Many of the most important advances concern “hard” materials, while applications to studying motions and relaxations of organic materials are restricted for many technical reasons.[2–4] Here, we are interested in transmission electron microscopy (TEM) of organic molecules in water. We report that synthetic polymers can be imaged in real time for periods up to 10–100 s using an ordinary TEM microscope whose kind is available to many researchers routinely.

There are two main impediments, in principle.[5] Dangers of sample damage are self-evident, as organic materials are notoriously sensitive to electron irradiation[6] and similarly, the water tends to decompose to form gas bubbles.[7] Second, in contrast to “hard” materials such as nanoparticles comprised of atoms whose atomic number is high,[8] electron scattering by carbon in organic materials is relatively weak.[9,10] Graphene windows are promising candidates for TEM imaging of organic molecules in liquid; they should be thin and thickness of the confined solutions should be small, in order to enhance the needed contrast by remaining translucent to illumination.[11,12] Graphene is impermeable to small-molecule liquids and its thermal and electrical conductivity appear to retard damage from electron irradiation such as heating, charging, and ionization.[13] Our study extends the liquid-cell TEM approach in which contrast is enhanced by confining the sample between ultrathin windows using various possible protocols, not only graphene but also silicon nitride.[14] The use of in situ liquid TEM has been demonstrated in recent past for visualizing structures of a variety of soft systems including virus,[9] liposomes,[15] aggregates of polymers,[16] and soft materials labeled with metal ions that provide contrast,[3,17,18] but not previously to individual polymer molecules in solution. Here, we have adapted a protocol that minimizes electron scattering[19] by using sheets as thin as practical to image polymers without metal-ion labeling, and we investigate their dynamics.

Our liquid pockets are constructed by laying one graphene sheet on top of a bottom graphene sheet to carefully produce creases in the top sheet that traps the liquid (for details, see Figure S1 in the Supporting Information). The needed mechanical integrity is provided by supporting the bottom on a TEM grid with holey carbon. Holey carbon adheres to graphene, which is traditional in electron microscopy, and we avoid the practice of also using holey carbon for the top sheet. Specifically, using commercial graphene (ACS Materials), we use 2-layer graphene for the bottom and 3–5-layer graphene for the top, as this combination gives the required stability[12] as well as contrast. First, we transfer CVD-grown graphene from copper foil onto a holey carbon gold TEM grid (QUANTIFOIL, Electron Microscopy Sciences and SPI Supplies). Onto it, we deposit by micropipette a relatively large liquid volume to maximize chances of forming multiple liquid pockets (about 0.5 μL), usually 1 wt% polymer in aqueous solution. Using tweezers,

Dr. K. H. Nagamanasa, Dr. H. Wang, Prof. S. Granick
IBS Center for Soft and Living Matter
UNIST
Ulsan 689-798, South Korea
E-mail: sgranick@ibs.re.kr

Prof. S. Granick
Departments of Chemistry and Physics
UNIST
Ulsan 689-798, South Korea

The ORCID identification number(s) for the author(s) of this article can be found under https://doi.org/10.1002/adma.201703555.

DOI: 10.1002/adma.201703555

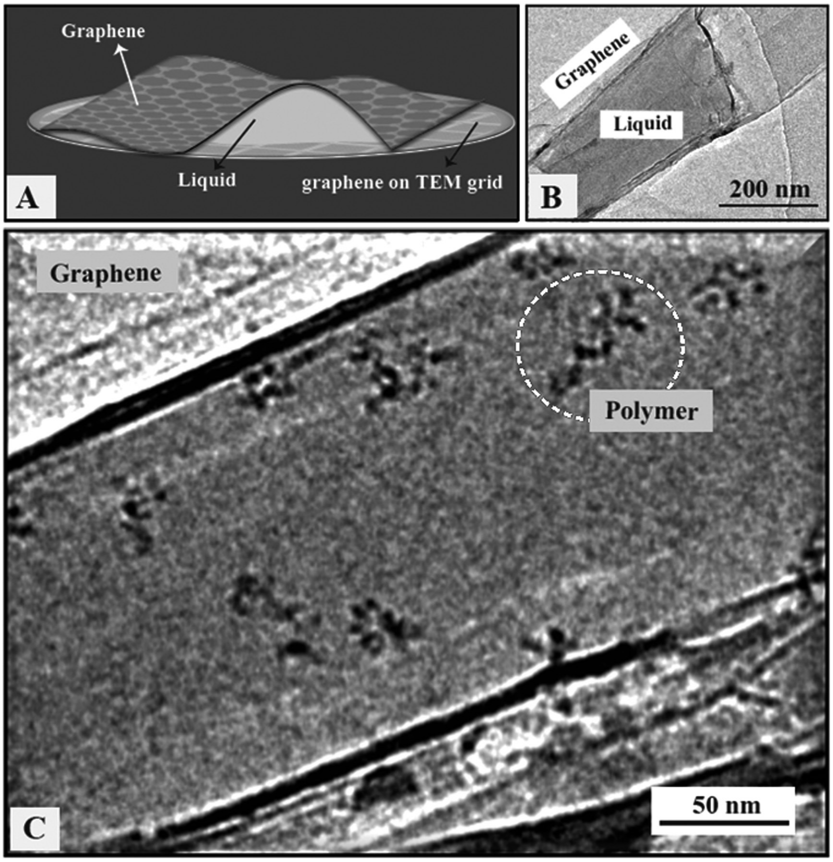

Figure 1. Experimental setup and representative data. A) Schematic of polymer solution sandwiched between graphene sheets. B) Large-area TEM image showing a representative liquid channel. For this low-magnification image, 1 pixel is 2.25 nm. C) TEM image showing individual polymer molecules, PSS, Polymer A in 0.2 M NaCl.

we gently place the graphene-coated grid onto a graphene sheet that floats on aqueous solution that etches away the copper, 0.1 M $(NH_4)_2S_2O_8$, and leave it for a few minutes. The graphene layers adhere strongly.[20] The waiting gives time to ensure good contact, thereby encapsulating the sample liquid between creases. **Figure 1**A shows a schematic diagram of the resulting liquid pocket.

Initial findings using polystyrene sulfonate (PSS) caused us to suspect that the relatively high atomic number of the sulfur might contribute to giving the needed contrast, but this turns out to be not essential as poly(ethylene oxide) (PEO) was also imaged, showing that the capability is more general. Our study includes three samples. First, PSS with weight-average molar mass $M_\mathrm{w} = 2200$ kDa (Polymer Source, $M_\mathrm{w}/M_\mathrm{n} = 1.15$). Second, PSS with weight-average molar mass 1030 kDa (Polymer Source, $M_\mathrm{w}/M_\mathrm{n} = 1.12$). Third, PEO with weight-average molar mass $M_\mathrm{w} = 2000$ kDa (Sigma-Aldrich). These we refer to below as Polymers A, B, and C, respectively. Normally, they are dissolved in deionized water at 10 mg mL^{-1} concentration but in control experiments, we also study Polymer A in 200×10^{-3} M NaCl. The experiments were performed, with an instrumental point resolution of 0.2 nm, on a JEOL-1400 TEM in the Central Research Facilities at our university. The 120 keV electron beam was calibrated to give a dose rate of 22 e $\text{Å}^{-2}\ \mathrm{s}^{-1}$, similar to that used by other researchers to study dynamics.[21] In the TEM images presented below, unless otherwise specified, 1 pixel is 0.74 nm.

Our sample preparation method gives a wide distribution of liquid pocket sizes with length usually larger than width. The typically rectangular shape illustrated in Figure 1B differs distinctly from the curved perimeter one might have anticipated naively, perhaps reflecting graphene's stiffness. In what follows below, our quantification considers only pockets that are relatively wide, wider than ≈150 nm and we refer to them as channels. The channel height is not known (we attempted unsuccessfully to measure it by imaging fluorescent markers) but is believed to be less than the width, and thinner close to the edges than at the center. This may encourage adsorption that is necessary for imaging on the time scale of hundreds of milliseconds. Remarkably, when we magnify one of these channels, images reveal objects that we interpret to be individual polymer molecules (Figure 1C). They are most often observed in channels wider than ≈150–200 nm and can be imaged for about ≈60 s before obvious degradation, while the channel itself can be imaged for 200 s before gas bubbles grow to fill the channels. It is common to find channels devoid of bubbles for 20 s, yet with molecules visible inside. While our statistical analysis finds that even with the subsequent growth of bubble size, the objects we interpret as polymer molecules are unaffected by the presence or absence of gas bubbles, we have not been able to determine firmly whether conformational rearrangement dynamics are influenced. They are useful practically as bubbles tend to reduce the thickness of remaining aqueous solution through which the electron beam traverses. This, we find, helps to enhance contrast.[4] In addition, bubble growth can concentrate molecules as the growing bubble sweeps through solution (Movie S1, Supporting Information).

It is not practical to analyze these systems for polymer by elemental characterization[17,22] (electron energy-loss spectroscopy (EELS) or energy-dispersive spectroscopy (EDS)), as polymer conformation changes are too rapid and anyway the required high electron energy would cause sample degradation. We chose the route of direct visualization instead, contrasting the images across different kinds of polymers, molecular weights, and even salt concentration. The images were acquired using a conventional charge coupled detector (CCD) (see Supporting Information). The images are 2D projections of 3D flexible coils and therefore show what appears to be branched structure, as illustrated in Figure 1C, whose dark spots indicate high electron scattering intensity on the experimental time scale. The dark spots probably reflect in part a large mass in 2D projection, in part that other regions with more rapid polymer segment mobility are blurred on the experimental time scale, resulting in lower contrast. Atomic force microscopy of adsorbed polymers shows dark spots and branched structures that qualitatively look similar.[23] Notably, the electron scattering contrast of PSS molecules (Figure 1C) and PEO molecules (**Figure 2**A) also looks similar. Charge on our PSS polyelectrolyte chains does not seem to be decisive, as we observed almost the same contrast for PEO chains, and they are uncharged. Furthermore, comparing contrast coming from PSS chain in solutions with and without salt, the contrast of Polymer A in deionized water is higher than in 0.2 M salt solution (see Figure S4 in the Supporting Information). This indicates that salt in the surrounding medium reduces the contrast as expected but does not alter polymer contrast directly. These polymers diffuse more sluggishly than in free solution where the longest relaxation time would be ≈0.1 ms,[24] more than three orders of magnitude faster than the frame rate of these measurements, but it is reasonable that these polymers tend to adsorb on the level of each segment to graphene, as graphene favors noncovalent adsorption from π–π van der Waals interactions and hydrophobic interactions[25] or even possible chemisorption as suggested by a recent study.[26]

Theories of polymer adsorption predict that when the segmental sticking energy is uniform for every segment, dilute polymers adsorb as flattened "pancakes,"[27] but this we do not observe. The discrepancy suggests segmental sticking energy so weak that these molecules are at the cusp between adsorption and desorption, which is also predicted.[28] Weak segmental sticking energy is consistent with conformation rearrangements and adsorption–desorption events that we report here, but we cannot at this time exclude the possibility that adsorption is assisted by some kind of chemical changes from interaction with incident electrons.

Illustrative images are shown not only for PSS but also for PEO in Figure 2A. The sizes of the molecules we observe are less than the anticipated radius of gyration ($R_g \approx 30$–50 nm) for chains of this molar mass in free solution, but the polydisperse molar mass gives big uncertainty to estimate of that quantity. Recognizing that this method of imaging selectively reveals the sluggish portions of adsorbed chains, we have computed the equivalent to R_g, the "pixel span" P_s (see Supporting Materials and Figure S5 in the Supporting Information), finding $P_s \approx 20$ nm. Statistical analysis from ≈35–40 molecules of each sample and 5 frames for each one, randomly chosen from the time series, gives us the distributions of P_s in Figure 2B for PSS (Polymers A with and without salt and also Polymer B) and Figure S6 in the Supporting Information (PEO). Relative probability plotted against P_s. In Figure 2B, the peak of the distribution shifts to a smaller value with decreasing molecular weight and increasing salt concentration, which makes physical sense. This quantification supports the interpretation that individual polymer molecules are observed. Further, discriminating the size distribution of different molecules in the polydisperse sample (Figure S7, Supporting Information) shows that the broad P_s distribution reflects the polydisperse molecular weight.

Figure 3A shows typical findings when the same polymer molecule was imaged for 70 s. For technical reasons, our measurements are separated in time by 1 s though the exposure time for each image is 0.3 s. In addition to the pixel span P_s just introduced, it is also relevant to quantify pixel count P_c which is believed to be proportional to the area of adsorbed segments.

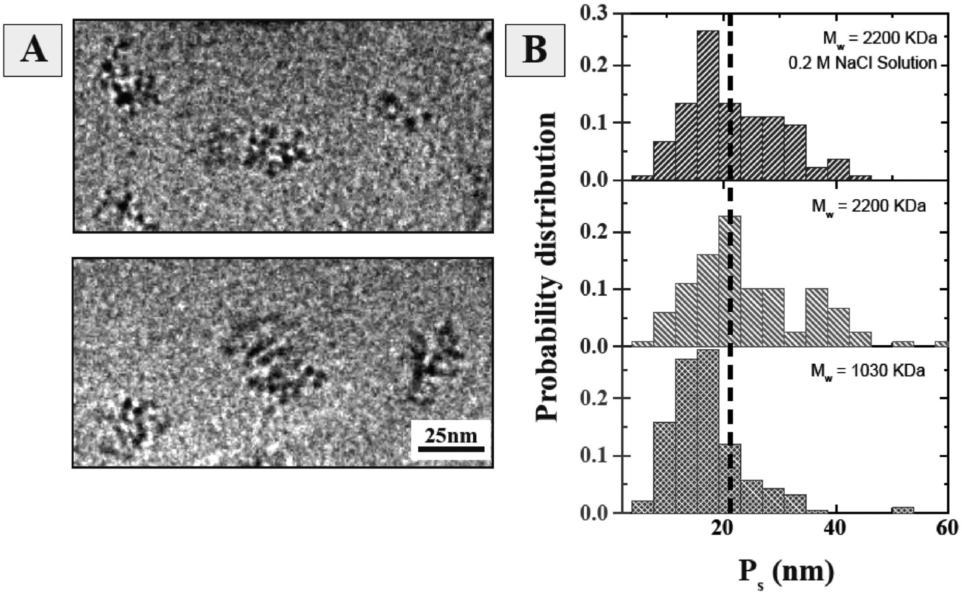

Figure 2. Size quantification. A) Representative images for PEO (top) and PSS Polymer A (bottom) in deionized water. B) Probability distributions compared for Polymer A in 0.2 M NaCl (top), deionized water (middle), and Polymer B in deionized water (bottom). The ordinate is pixel span P_s, which is the analogue of radius of gyration filtered by this experiment's selection of observables that are visible on only the experimental time scale of 0.3 s. The distributions have been normalized by total number of events which are 135, 119, and 190 for these three cases, respectively. The dotted vertical line in (B) shows that relative to the peak of the distribution in the middle panel, the peak is less in salt solution and also for a sample of lower molecular weight.

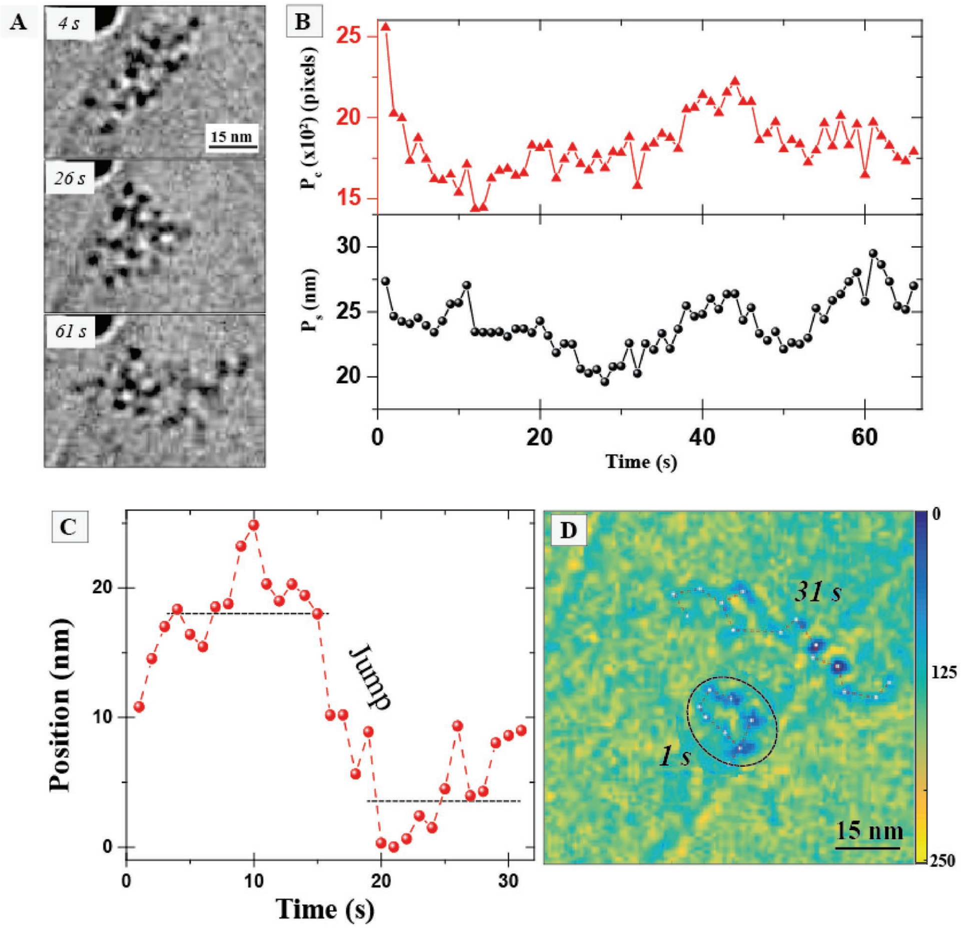

Figure 3. Conformational rearrangements and adsorption–desorption. A) With exposure time 0.3 s per frame, the images show snapshots of a molecule of Polymer A at three different times indicated in the panel. B) Quantifying the images in panel A, the pixel count P_c and pixel span P_s are plotted against time for 65 s. C) The center-of-mass position in the laboratory frame of reference is plotted against time for a molecule of Polymer A for 30 s, with exposure time 0.3 s per frame and 1 s between frames. The position shifts by ≈20 nm over a few seconds, probably reflecting partial detachment and readsorption (a "jump"). Fluctuations of center-of-mass position before and after these times are believed to reflect conformational changes. D) These images contrast snapshots of the molecule in Panel C at times 1 s and 31 s. The image is color coded according to intensity as shown in the color bar.

Movie S2 in the Supporting Information illustrates these fluctuations. In Figure 3A, one notices that the magnitudes of conformational fluctuations (P_s) are almost the same as those of fluctuations in the number of adsorbed segments (P_c); their standard deviations are 9% and 10%, respectively. These time series are illustrated in Figure 3B. This makes sense physically; adsorbed molecules fluctuate but without exploring the full range of probability distribution. Within a range of fluctuation in the adsorbed state, they tend to stick where they land.

The alternative pessimistic hypothesis of radiation damage must be considered. The critical cumulative electron dose has been studied for films of undiluted polymers[29] giving numbers on the order of 50 C m^{-2} (polystyrene)[30] and 0.01 C m^{-2} (PEO).[31] Comparing to our experiments by converting units and considering typical lifetime ≈60 s gives an estimated electron dose of 200 C m^{-2} in our experiments. The similar order of magnitude is pleasing, considering the different environmental conditions of liquid and graphene-rich environment. It is true that events of radiation damage are observed directly from time to time after relatively long exposure to electrons (see Supporting Information section on radiation effects, Figure S8, and Movie S3). Specifically, Figure S8A,B in the Supporting Information illustrates two processes, chain scission and recombination, expected from knowledge of radiation processing of polymers,[29,32] observed here for two molecules at times ≈45 and ≈125 s (Movie S3, Supporting Information). But while we have no direct information whether radiation damage stimulates adsorption, if this were so we would anticipate adsorption to be irreversible, not reversible as we observe. Molecules sometimes detach from the surface, then re-adsorb. The molecule illustrated in Figure 3C and Movie S4 in the Supporting Information first enjoys conformational fluctuations that produce slight fluctuations of its center-of-mass position, then it "jumps" to a new adsorbed position on the graphene sheet, followed by a new sequence of conformational fluctuations. The jump event is accompanied by a coil-to-stretch conformational transition (Figure 3D) that we consider to be coincidental. Elsewhere using fluorescence imaging in a different system, we considered this kind of polymer adsorption–desorption event in detail.[33]

Recalling that this experiment filters images such that only long-lived adsorption states are observed, adsorption of a polymer molecule is illustrated in Figure S9A and Movie S5 in the Supporting Information. Figure S9B in the Supporting Information plots against time the increasing pixel counts (P_c), which we interpret as proportional to the number of polymer segments adsorbed on the observational time window; this number rises from zero and saturates at a plateau followed only by conformational changes that cause P_s to fluctuate. TEM cameras with higher time resolution[34] would enable better resolution of the kinetics of this process.

In summary, objects that we interpret as single polymer molecules have been imaged by TEM microscopy in liquid-cell environment. Confirming that the objects observed here are polymers, we find that size of these objects changes rationally according to molecular weight and salt concentration. Other characteristic features of individual coiled polymer molecules are also confirmed, including conformational changes, adsorption–desorption, and patterns of radiation damage involving chain scission and recombination. These experiments were performed using routine TEM equipment. The alleviation of ordinarily expected sample degradation by confinement in a graphene liquid cell opens opportunities for advances in imaging organic materials of other kinds, not only synthetic polymers but also naturally occurring polymers such as DNA and proteins.

Supporting Information

Supporting Information is available from the Wiley Online Library or from the author.

Acknowledgements

K.H.N. and H.W. contributed equally to this work. The authors thank taxpayers who supported this work through the Korean Institute for Basic Science, project code IBS-R020-D1. For discussions, the authors are indebted to Qian Chen, Oh-Hoon Kwon, Ye-Jin Kim, and Cong Xu.

Conflict of Interest

The authors declare no conflict of interest.

Keywords

adsorbed polymers, graphene liquid cells, imaging, in situ liquid TEM

Received: June 26, 2017
Revised: August 5, 2017
Published online:

---

[1] F. Balzarotti, Y. Eilers, K. C. Gwosch, A. H. Gynnå, V. Westphal, F. D. Stefani, J. Elf, S. W. Hell, *Science* **2017**, *355*, 606.

[2] H. Zheng, R. K. Smith, Y.-W. Jun, C. Kisielowski, U. Dahmen, A. P. Alivisatos, *Science* **2009**, *324*, 1309.

[3] J. P. Patterson, M. T. Proetto, N. C. Gianneschi, *Perspect. Sci.* **2015**, *6*, 106.

[4] N. De Jonge, F. M. Ross, *Nat. Nanotechnol.* **2011**, *6*, 695.

[5] F. M. Ross, *Liquid Cell Electron Microscopy*, Cambridge University Press, Cambridge, UK **2016**.

[6] L. Reimer, *Transmission Electron Microscopy: Physics of Image Formation and Microanalysis*, Vol. *36*, Springer-Verlag, Heidelberg, Germany **2013**.

[7] a) N. M. Schneider, M. M. Norton, B. J. Mendel, J. M. Grogan, F. M. Ross, H. H. Bau, *J. Phys. Chem. C* **2014**, *118*, 22373; b) J. M. Grogan, N. M. Schneider, F. M. Ross, H. H. Bau, *Nano Lett.* **2013**, *14*, 359.

[8] a) J. M. Yuk, J. Park, P. Ercius, K. Kim, D. J. Hellebusch, M. F. Crommie, J. Y. Lee, A. Zettl, A. P. Alivisatos, *Science* **2012**, *336*, 61; b) H.-G. Liao, K. Niu, H. Zheng, *Chem. Commun.* **2013**, *49*, 11720.

[9] A. C. Varano, A. Rahimi, M. J. Dukes, S. Poelzing, S. M. McDonald, D. F. Kelly, *Chem. Commun.* **2015**, *51*, 16176.

[10] M. T. Proetto, A. M. Rush, M.-P. Chien, P. Abellan Baeza, J. P. Patterson, M. P. Thompson, N. H. Olson, C. E. Moore, A. L. Rheingold, C. Andolina, *J. Am. Chem. Soc.* **2014**, *136*, 1162.

[11] a) M. Wojcik, M. Hauser, W. Li, S. Moon, K. Xu, *Nat. Commun.* **2015**, *6*, 7384; b) R. Nair, P. Blake, J. Blake, R. Zan, S. Anissimova, U. Bangert, A. Golovanov, S. Morozov, A. Geim, K. Novoselov, *Appl. Phys. Lett.* **2010**, *97*, 153102; c) U. Mirsaidov, V. Mokkapati, D. Bhattacharya, H. Andersen, M. Bosman, B. Özyilmaz, P. Matsudaira, *Lab Chip* **2013**, *13*, 2874; d) Q. Chen, J. M. Smith, J. Park, K. Kim, D. Ho, H. I. Rasool, A. Zettl, A. P. Alivisatos, *Nano Lett.* **2013**, *13*, 4556.

[12] J. Park, H. Park, P. Ercius, A. F. Pegoraro, C. Xu, J. W. Kim, S. H. Han, D. A. Weitz, *Nano Lett.* **2015**, *15*, 4737.

[13] R. Zan, Q. M. Ramasse, R. Jalil, T. Georgiou, U. Bangert, K. S. Novoselov, *ACS Nano* **2013**, *7*, 10167.

[14] a) A. S. Powers, H.-G. Liao, S. N. Raja, N. D. Bronstein, A. P. Alivisatos, H. Zheng, *Nano Lett.* **2017**, *17*, 15; b) N. D. Loh, S. Sen, M. Bosman, S. F. Tan, J. Zhong, C. A. Nijhuis, P. Král, P. Matsudaira, U. Mirsaidov, *Nat. Chem.* **2017**, *9*, 77.

[15] S. M. Hoppe, D. Y. Sasaki, A. N. Kinghorn, K. Hattar, *Langmuir* **2013**, *29*, 9958.

[16] J. Liu, B. Wei, J. D. Sloppy, L. Ouyang, C. Ni, D. C. Martin, *ACS Macro Lett.* **2015**, *4*, 897.

[17] C. Wang, Q. Qiao, T. Shokuhfar, R. F. Klie, *Adv. Mater.* **2014**, *26*, 3410.

[18] L. M. DiMemmo, A. C. Varano, J. Haulenbeek, Y. Liang, K. Patel, M. J. Dukes, S. Zheng, M. Hubert, S. P. Piccoli, D. F. Kelly, *Lab Chip* **2017**, *17*, 315.

[19] Y. Sasaki, R. Kitaura, J. M. Yuk, A. Zettl, H. Shinohara, *Chem. Phys. Lett.* **2016**, *650*, 107.

[20] J. M. Yuk, K. Kim, B. Alemán, W. Regan, J. H. Ryu, J. Park, P. Ercius, H. M. Lee, A. P. Alivisatos, M. F. Crommie, *Nano Lett.* **2011**, *11*, 3290.

[21] a) U. M. Mirsaidov, H. Zheng, D. Bhattacharya, Y. Casana, P. Matsudaira, *Proc. Natl. Acad. Sci.* **2012**, *109*, 7187; b) J. Kim, M. R. Jones, Z. Ou, Q. Chen, *ACS Nano* **2016**, *10*, 9801.

[22] M. E. Holtz, Y. Yu, J. Gao, H. D. Abruña, D. A. Muller, *Microsc. Microanal.* **2013**, *19*, 1027.

[23] Y. Roiter, O. Trotsenko, V. Tokarev, S. Minko, *J. Am. Chem. Soc.* **2010**, *132*, 13660.

[24] M. Rubinstein, R. H. Colby, *Polymer Physics*, Oxford University Press, Oxford, UK **2003**.

[25] a) K. P. Loh, Q. Bao, P. K. Ang, J. Yang, *J. Mater. Chem.* **2010**, *20*, 2277; b) V. Georgakilas, M. Otyepka, A. B. Bourlinos, V. Chandra, N. Kim, K. C. Kemp, P. Hobza, R. Zboril, K. S. Kim, *Chem. Rev.* **2012**, *112*, 6156.

[26] S. Böttcher, H. Vita, M. Weser, F. Bisti, Y. Dedkov, K. Horn, *J. Phys. Chem. Lett.* **2017**, *8*, 3668.
[27] S. A. Sukhishvili, Y. Chen, J. D. Müller, E. Gratton, K. S. Schweizer, S. Granick, *Nature* **2000**, *406*, 146.
[28] G. Forgacs, V. Privman, H. Frisch, *J. Chem. Phys.* **1989**, *90*, 3339.
[29] J. E. Mark, *Physical Properties of Polymers Handbook*, Vol. *1076*, Springer, New York **2007**.
[30] K. Varlot, J. Martin, C. Quet, *J. Microsc.* **1998**, *191*, 187.
[31] P. Krsko, S. Sukhishvili, M. Mansfield, R. Clancy, M. Libera, *Langmuir* **2003**, *19*, 5618.
[32] A. G. Chmielewski, M. Haji-Saeid, S. Ahmed, *Nucl. Instrum. Methods Phys. Res., Sect. B* **2005**, *236*, 44.
[33] C. Yu, J. Guan, K. Chen, S. C. Bae, S. Granick, *ACS Nano* **2013**, *7*, 9735.
[34] Y. M. Lee, Y. J. Kim, Y.-J. Kim, O.-H. Kwon, *Struct. Dyn.* **2017**, *4*, 044023.